Critical slowing down of the Amazon forest after increased drought occurrence

Van Passel, Johanna; Bernardino, Paulo N.; Lhermitte, Stef; Rius, Bianca F.; Hirota, Marina; Conradi, Timo; de Keersmaecker, Wanda; Van Meerbeek, Koenraad; Somers, Ben

DOI
10.1073/pnas.2316924121

Publication date
2024

Document Version
Final published version

Published in
Proceedings of the National Academy of Sciences of the United States of America

Citation (APA)
Van Passel, J., Bernardino, P. N., Lhermitte, S., Rius, B. F., Hirota, M., Conradi, T., de Keersmaecker, W., Van Meerbeek, K., & Somers, B. (2024). Critical slowing down of the Amazon forest after increased drought occurrence. *Proceedings of the National Academy of Sciences of the United States of America*, *121*(22), e2316924121. Article e2316924121. https://doi.org/10.1073/pnas.2316924121

PNAS RESEARCH ARTICLE | ENVIRONMENTAL SCIENCES

Critical slowing down of the Amazon forest after increased drought occurrence

Johanna Van Passel[a,b,1], Paulo N. Bernardino[a,c], Stef Lhermitte[a,d], Bianca F. Rius[e,f], Marina Hirota[c,f], Timo Conradi[g], Wanda de Keersmaecker[h], Koenraad Van Meerbeek[a,b], and Ben Somers[a,b]

Edited by Stephen Carpenter, University of Wisconsin-Madison, Madison, WI; received October 5, 2023; accepted April 5, 2024

Dynamic ecosystems, such as the Amazon forest, are expected to show critical slowing down behavior, or slower recovery from recurrent small perturbations, as they approach an ecological threshold to a different ecosystem state. Drought occurrences are becoming more prevalent across the Amazon, with known negative effects on forest health and functioning, but their actual role in the critical slowing down patterns still remains elusive. In this study, we evaluate the effect of trends in extreme drought occurrences on temporal autocorrelation (TAC) patterns of satellite-derived indices of vegetation activity, an indicator of slowing down, between 2001 and 2019. Differentiating between extreme drought frequency, intensity, and duration, we investigate their respective effects on the slowing down response. Our results indicate that the intensity of extreme droughts is a more important driver of slowing down than their duration, although their impacts vary across the different Amazon regions. In addition, areas with more variable precipitation are already less ecologically stable and need fewer droughts to induce slowing down. We present findings indicating that most of the Amazon region does not show an increasing trend in TAC. However, the predicted increase in extreme drought intensity and frequency could potentially transition significant portions of this ecosystem into a state with altered functionality.

tropical forest | resilience | drought response

Significance

The increasing frequency and intensity of droughts in the Amazon rainforest raises concerns about potential forest dieback. However, the precise role of drought occurrences in this phenomenon remains unclear. We used trends in temporal autocorrelation of satellite-derived indices of vegetation activity as a proxy for the critical slowing down response of the Amazon and differentiated between drought frequency, intensity, and duration to investigate their respective effects on the slowing down response. We found that this slower recovery to perturbations prevails in regions experiencing more frequent, intense, and longer droughts, albeit with regional variations. Most of the Amazon does not show critical slowing down, but the predicted increase in droughts could disrupt this balance, signifying the importance of understanding these dynamics.

Tropical forests account for half of the global forest carbon sink, with the largest contribution coming from the Amazon forest (1, 2). The Amazon is also a biodiversity hotspot, with an estimated 15,000 tree species (3). However, recent studies observed critical slowing down of vegetation activity across the Amazon since the early 2000s (4–6). Theory suggests that critical slowing down, or the increasingly slower return rate from small perturbations (7), is an early warning indicator of dynamic systems approaching a critical threshold into an ecosystem state with different functioning. Ongoing climate change might be the driver of this push toward large-scale ecosystem collapse, but its precise association with recent extreme drought occurrences is unknown (8).

Over the past 20 y, the Amazon has experienced three "one-in-a-century droughts," and these extreme events are predicted to become more frequent and intense due to climate change (9–12). Previous research has already focused on the relationship between ecosystem stability and precipitation dynamics within the Amazon. Notably, areas experiencing lower rainfall showed the largest stability decline since the early 2000s (4), and droughts were found to be the primary driver of the 30-y decline in radar signal in a pantropical study (13). Moreover, more severe droughts were more likely to lead to a negative forest response (14). While progress has been made in understanding the impact of individual droughts on tropical forest stability, the question remains whether and how multiple of these pulse disturbances over an extended time frame result in slowing down of the Amazon forest vegetation. Depending on the drought severity and the diversity of life strategies within the affected communities, we would expect that recurring drought events would lead to reduced forest recovery rates due to a gradual decrease in tree growth and increase in tree mortality (15), potentially leading the forest community to cross a critical threshold. Furthermore, the expected negative impact of recurrent extreme droughts and more specifically the relative importance of different aspects of drought occurrences—frequency, intensity, and duration—on the slowing down response of the Amazon forest vegetation have never been quantified on a large scale (16).

Increased temporal autocorrelation (TAC) in the time series of a system's state variable can be used as an indicator for slowing down (7). TAC quantifies the level of correlation between consecutive time points in a time series representing an ecosystem. As TAC increases, the ecosystem's current state is more similar to its previous state over time (5, 17, 18). This method has been used successfully to detect critical slowing down near

The authors declare no competing interest.

This article is a PNAS Direct Submission.

[1]To whom correspondence may be addressed. Email: johanna.vanpassel@kuleuven.be.

This article contains supporting information online at https://www.pnas.org/lookup/suppl/doi:10.1073/pnas.2316924121/-/DCSupplemental.

Published May 20, 2024.

ecological thresholds (7, 19). In tropical forests, both static stability and its temporal variations have been assessed using TAC (4, 5, 20, 21). Another potential indicator of slowing down is a corresponding increase in the variance of the system's state time series (22). However, this variance increase is less reliable than the increase observed in TAC leading up to a critical transition (18, 20).

In this study, we investigate whether recurrent extreme drought events, particularly variations in their frequency, intensity, or duration, contribute to stability loss of the Amazon vegetation due to critical slowing down. As the concept of critical speeding up, a theoretical alternative for detecting stochastically driven critical transitions, has been proposed as another mechanism that could decrease stability, we explored the possibility of critical speeding up occurring. Nevertheless, our investigation did not yield any evidence supporting critical speeding up (*SI Appendix*, Text). To quantify critical slowing down, we use TAC trends estimated from satellite-derived time series of vegetation activity (*Materials and Methods*). We first derive the TAC over native vegetation pixels as the lag-1 autocorrelation of monthly Moderate Resolution Imaging Spectrometer (MODIS) Enhanced Vegetation Index (EVI) time series from 2001 to 2019 with a spatial resolution of 5×5 km^2 (23). EVI functions as a proxy for canopy productivity and greenness in tropical forests (24), and TAC derived from EVI and from similar greenness indices has been used as an indicator of (tropical) forest mortality (19, 20, 25). More intense and longer extreme droughts were also correlated with a more substantial decrease in EVI during the year following the drought across the Amazon forest (*SI Appendix*, Fig. S1). Then, we explore the link between slowing down and extreme drought occurrences using cumulative water deficit (CWD) anomalies derived from precipitation time series (14, 26) (*Materials and Methods*).

Results

General Trends across the Amazon Forest. The Amazon-wide analysis of EVI TAC shows that 37% of the mature vegetation exhibited slowing down, corresponding to an overall increasing linear trend in TAC over the past 20 y, with a large spatial variability in the trends across the Amazon forest (Fig. 1). In general, the trends increase from the northwest to the southeast (*SI Appendix*, Table S1), following the overall rainfall gradient present throughout the Amazon basin. This gradient implies a generally higher vulnerability of the south-eastern Amazon to a tipping event.

The mean EVI TAC time series over the whole Amazon forest shows a significant decreasing trend until halfway 2014, followed by a significant increasing trend up to 2019 (Fig. 1). Varying the window length from five to three or seven years to calculate the TAC gives similar temporal and spatial results (*Materials and Methods* and *SI Appendix*, Fig. S2). We also compared the EVI TAC trend with the TAC trends of vegetation optical depth [VOD, spatial resolution of 25×25 km^2, based on earlier analysis of Boulton et al. (4), although there are some known issues with this dataset (27)] and kernel Normalized Difference Vegetation Index [kNDVI, spatial resolution of 5×5 km^2, less sensitive to saturation than EVI (28)]. All three indices show similar spatial and temporal patterns indicating that the different EVI, VOD, and kNDVI vegetation proxies have comparable results in terms of slowing down, even though they represent changes in canopy greenness, vegetation structure, and gross primary productivity, respectively (*Materials and Methods* and *SI Appendix*, Figs. S3 and S4). However, we focus further analyses of this study on the finer-scale EVI TAC trend (but showing the kNDVI model results in *SI Appendix*, *Materials*), as fine-scale ecosystem heterogeneity plays an important role in tropical forest mortality to drought (25, 29, 30).

Impact of Extreme Drought Frequency, Intensity, and Duration. Earlier studies have demonstrated EVI's sensitivity to extreme drought occurrences (*SI Appendix*, Fig. S1 and refs. 14 and 24). Building upon this, we initially assessed the sensitivity of the EVI TAC to extreme drought occurrences by comparing the average time series across all pixels that experienced the widespread drought events in 2005, 2010, and 2015 and the mean TAC trends between pixels with different drought history categories (*Materials and Methods* and *SI Appendix*, Figs. S5 and S6). Subsequently, we analyzed the potential drivers of this slowing down of the Amazon forest vegetation by exploring its relationship with extreme drought occurrences. Therefore, we implemented Spatial Simultaneous Autoregressive Lag Models (SSALMs) to account for spatial autocorrelation in the data (31) (*Materials and Methods*). The trend in TAC was used as the response variable, while multiple drought and environmental characteristics were included as explanatory variables (*Materials and Methods*, Fig. 2, and *SI Appendix*, Fig. S7 and Table S2). In all analyses, coefficients showing significant positive effects on the TAC trend are considered to have a destabilizing effect on the ecosystem, since they contribute to an increase in TAC over time, potentially leading to slowing down of the ecosystem.

The SSALM results first show a destabilizing effect for different drought characteristics. An increase in both the intensity and duration of extreme droughts has a significant positive impact on the trend of TAC, leading to slowing down within the ecosystem (Fig. 2 and *SI Appendix*, Table S2). Our results indicate that while the main effect of drought frequency is not significant, its interaction with drought intensity significantly increases the TAC trend. Furthermore, our findings confirm previous research which suggests that wet periods could help to stabilize an ecosystem in the face of increased droughts (14, 32) (*SI Appendix*, Fig. S7 and Table S2). When we i) extend the studied drought period up to 15 y earlier, ii) use different moving window lengths to calculate the TAC, iii) include only the pixels with a significant TAC trend when in agreement with the SD trend (5) (*Materials and Methods* and *SI Appendix*, Fig. S8), or iv) use the kNDVI TAC trend instead of the EVI TAC trend, the models show consistent destabilizing effects of extreme drought occurrences on the TAC trend. The models explain a limited part of the variation in the TAC trend, showing pseudo-R^2 values between 0.08 and 0.14 (*SI Appendix*, Tables S2–S5). These relatively low values align with other recent research investigating the effects of droughts on tropical forests (33, 34), and are partly caused by the large variation within pixels and the lack of detailed information on soil moisture, texture, and tree species composition. Moreover, the factors that influence the trends in TAC were found to vary across different regions within the Amazon forest. We repeated the analysis for 13 different woody plant subregions within the Amazon (35) (*Materials and Methods*, Fig. 3, and *SI Appendix*, Table S1). In the north-western Amazon, an increase in the TAC trend is solely attributed to more frequent extreme droughts and higher climate variability. However, in the southern and north-eastern Amazon, longer and/or higher intensity droughts also contribute to the increase in the TAC trend (Fig. 3 and *SI Appendix*, Table S1).

The Amazon forest is a complex system, which cannot be completely captured using only one parameter such as lag-1 autocorrelation in EVI time series. The critical slowing down theory is developed to understand tipping points induced by bifurcation in one-dimensional systems, therefore requires careful application

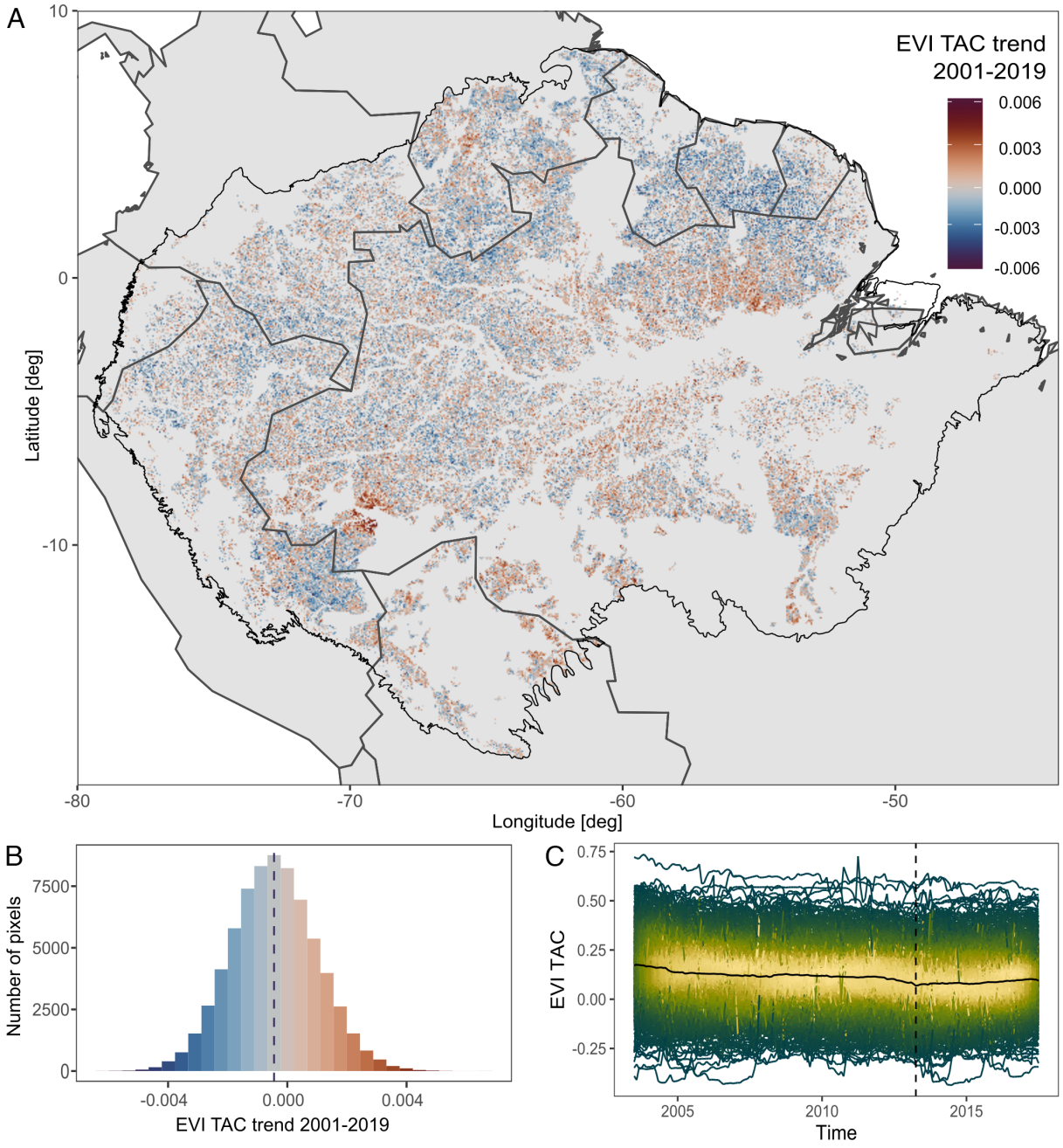

Fig. 1. General trends in EVI TAC across the Amazon forest. (*A*) EVI TAC trend from January 2001 until December 2019 across the Amazon forest. (*B*) Frequency distribution of the EVI TAC trend across the Amazon with the dashed line showing the mean trend value. (*C*) Mean EVI TAC time series from July 2003 until July 2017 across the Amazon forest (black line) with the density of the TAC time series of 1,000 random pixels shown from dark green to yellow (with density values ranging between 1 and 250). In (*C*), the values are plotted in the middle of the five-year moving window, and the lowest mean TAC value occurs in April 2013 (dotted line), with the mean trend from July 2003 until April 2013 and the total trend significantly negative and the mean trend from April 2013 until July 2017 significantly positive.

in a system that might be represented by more dimensions (36). In further support of our interpretation regarding the Amazon's diminishing stability due to increased drought occurrences, we employed a Bayesian dynamic linear model (DLM) to estimate time-varying EVI TAC, while also accounting for the variation in climate forcing (ref. 37 and *Materials and Methods*). Echoing the results of the conventional TAC metric, the trend of this time-varying TAC also displayed an increase with longer drought histories (*SI Appendix*, Fig. S9).

Effect of Precipitation Regime. The SSALM also shows a strong impact of the precipitation regime on the slowing down response of the Amazon, as both precipitation seasonality and the interannual variability of the precipitation determine the rate of slowing down. Our results show that a greater degree of seasonality (i.e., concentrated precipitation within a shorter rainy season, calculated as the Seasonality Index from Walsh and Lawler (38) and *Materials and Methods*) and a higher interannual variability of precipitation (i.e., more variable rainfall between years, calculated as the coefficient of variation of the annual mean precipitation values (39) and *Materials and Methods*) have a negative impact on the stability of tropical forests, and this impact gets more negative when the area experienced more droughts (*SI Appendix*, Fig. S7 and Tables S2–S5). These negative effects of more variable precipitation on the trend in TAC are consistent across most of the 13 subregions within the Amazon forest (*SI Appendix*, Table S1).

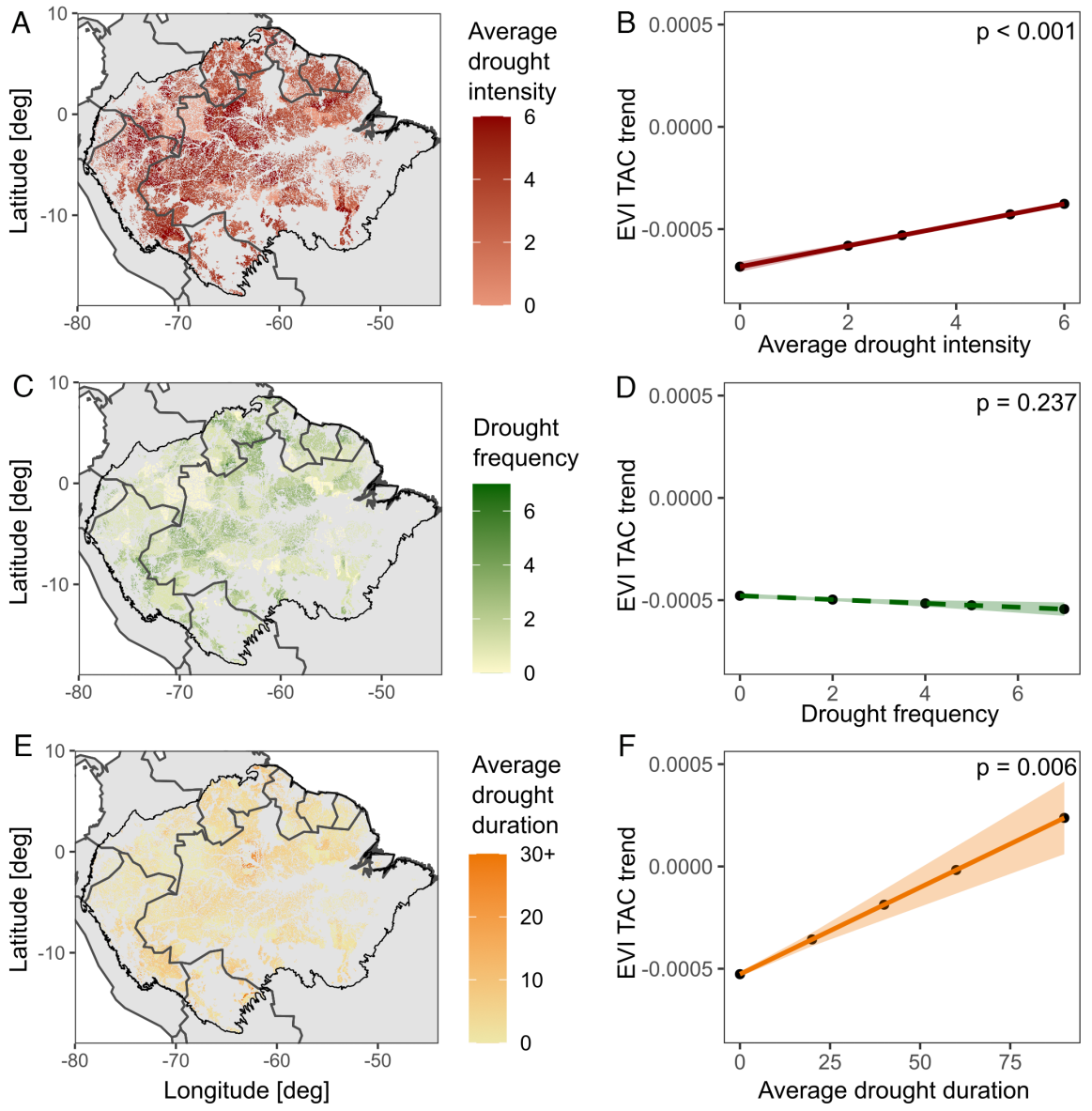

Fig. 2. Patterns of drought-related drivers of critical slowing down in the Amazon forest (*Left* column) and their marginal effects on the EVI TAC trend in the Amazon-wide Spatial Simultaneous Autoregressive Lag Model (*Right* column, *SI Appendix*, Table S2). A marginal effect is the predicted change in the EVI TAC trend after varying a variable of interest while holding others constant at their mean value. (*A* and *B*) Average drought intensity (i.e., most negative cumulative water deficit value); (*C* and *D*) drought frequency (i.e., number of occurred droughts); and (*E* and *F*) average drought duration (i.e., number of drought months) across the Amazon forest. The main effect of drought frequency on the TAC trend was not significant in the Amazon-wide model.

Discussion

We find that more than one-third of the investigated forest area of the Amazon shows an increasing trend in EVI TAC of their canopy productivity over the period between 2001 and 2019. Given EVI's capability to detect changes in forest functioning in the Amazon (24), this increasing trend could be considered an early warning indicator that these areas are approaching a threshold to a die-off event, leading to an ecosystem state with qualitatively different functioning.

This slowing down in one-third (37%) of the Amazon is contradictive to the findings of Boulton et al. (4), whose research indicated that three-quarters (76%) of the Amazon showed slowing down by increasing trends in VOD TAC from 2003 onward. This difference in area affected by slowing down can partly be attributed to the different time periods used for the TAC calculations. When evaluated over the same time span (2001 to 2016), using VOD instead of EVI, only 50% of all VOD pixels show an increasing trend in TAC, compared to 38% of all EVI pixels (*SI Appendix*, Fig. S3). Moreover, both indices display similar mean TAC trends in our study, with a significant increase only starting in April 2012 and 2013 for VOD and EVI TAC, respectively. This one-year time lag between VOD and EVI TAC could be linked to the intrinsic properties of these indices. EVI only captures the response of photosynthetic vegetation, while VOD represents both photosynthetic and nonphotosynthetic biomass. When assessing the fire response of tropical forests, EVI was found to recover faster than VOD, possibly due to leaves responding more rapidly than branches (40, 41). This pattern of fast canopy recovery might extend to drought events, as suggested by *SI Appendix*, Fig. S1. The concept of critical slowing down points toward a slower recovery rate following perturbations, thus it would make sense that VOD shows this slowing down response earlier in the time series than EVI.

South-eastern Amazon forests exist under drier and more seasonal rainfall conditions and thus are likely to better cope with

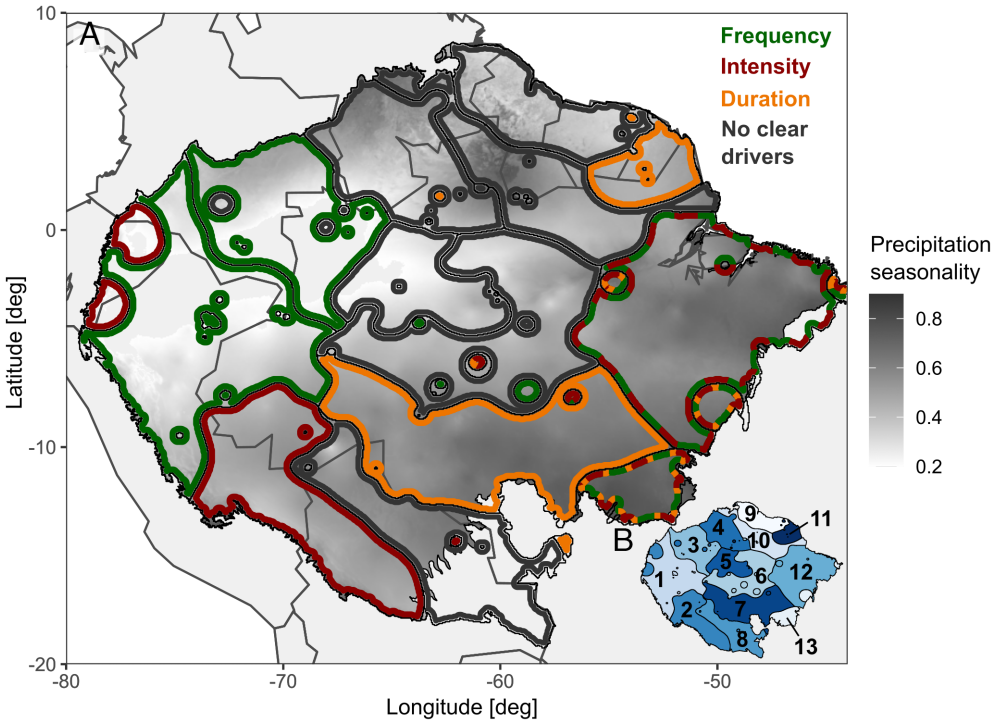

Fig. 3. Drought-related drivers of slowing down of the Amazon forest for each woody plant subregion, shown on top of the precipitation seasonality across the Amazon. (*A*) The colored outlines of the various subregions indicate whether drought frequency, intensity, duration, or none of these factors were significant drivers of slowing down in each region. Variables were defined as drivers of slowing down in a region when they had at least one significant increasing main or interaction effect on the TAC trend and no significant decreasing effects. (*B*) Woody plant subregions from Silva-Souza and Souza (35).

increasing drier conditions (39, 42). However, given that they are already operating at their physiological limits (43), they may be more vulnerable to shift than in western regions of the basin. This vulnerability has been shown previously using both modeled and coarse-scale satellite data (4, 16). Our results confirm this observation using finer-scale satellite imagery, and furthermore, link this increasing trend in TAC to areas that experienced a higher drought frequency, intensity, and duration. This causal relationship between extreme drought occurrences and slowing down is also supported by ecological evidence that extreme droughts can lead to forest mortality and thus ecosystem changes in structure and function (44, 45). Since drought frequency and intensity over the Amazon are predicted to increase with ongoing climate change (12), this implies that the effects of slowing down are expected to aggravate. In other words, more future droughts are expected to cause changes in forest structure and functioning by increasing forest mortality and can potentially bring more areas in the Amazon closer to a tipping point, especially those areas already more affected by climate change and land use changes.

Our results show moreover that the intensity of extreme drought events is more important than their duration for critical slowing down, as the standardized coefficient of drought duration is smaller than that of drought intensity in the Amazon-wide model, and not even significant in the combined TAC-SD model (Fig. 2 and *SI Appendix*, Tables S2, S4, and S5). This can be explained by the biological response of trees to droughts. Droughts can cause tree mortality through two pathways: hydraulic failure and carbon starvation (46). Hydraulic failure occurs when the water loss from transpiration exceeds the water uptake, causing xylem vessels to become embolized and reducing the tree's water transport capacity, ultimately leading to death. Carbon starvation occurs when a tree avoids hydraulic failure by closing its stomata and, leading to a negative carbon balance and death during prolonged periods without photosynthesis. High intensity droughts are more likely to cause irreversible dehydration, resulting in hydraulic failure, while longer low-intensity droughts can cause mortality through carbon starvation (46). Hydraulic failure has been proposed as the major trigger for tree mortality in tropical rainforests (44), which aligns with our findings that drought intensity increases the slowing down response more than drought duration.

Extreme wet precipitation events are also known to have negative effects on tree growth and survival (32). Our results did not show a significant effect of more severe extreme wet periods on the slowing down of the Amazon forest vegetation. However, we found a significant decreasing effect on the TAC trend when they occurred in combination with more droughts. This may indicate a buffering effect of the wet period's water excess which is stored in the groundwater and can maintain surface water bodies during following dry periods (14, 32). Within the regional models, this buffering effect is only significant in the north-eastern subregion 11.

We also find that a more variable precipitation pattern increases the slowing down of the Amazon forest, both on the scale of the whole Amazon and within all the regional models. These destabilizing effects could partly be explained by the fact that seasonality is negatively correlated with mean annual precipitation across the Amazon, and pantropical vegetation in wetter areas was found to have a lower TAC (20). Smith and Boers (21) also found that empirical recovery rates generally decreased with more concentrated precipitation in a global study. We did not find the previously suggested positive effect of high precipitation variability on the stability of tropical vegetation to droughts (39). However, the interannual variability of precipitation in this study was calculated over a period of 40 years, which cannot encompass the lifespan of a forest community. Other research that used a similar short-term period to define the interannual variability of precipitation did find the same negative relationship with vegetation stability, albeit on a global scale (21).

The spatial variability we found in response to the different types of droughts can be related to ecological differences in forest communities across the Amazon. In the Amazon forest, evergreen and (semi)deciduous tree species co-occur, but dry-affiliated species are more common in southern and central regions than in the northwest (47, 48). Previous research suggests that tropical forest communities are shifting toward more dry-affiliated and deciduous components with less rainfall, both through recruits that are more dry-affiliated and through higher mortality of wet-affiliated trees (42, 49). Furthermore, tree species found in more seasonal forests have progressively more resistant xylem tissue (43). The lower mean annual precipitation and higher seasonality of the south-eastern region (woody subregions 7 and 13; Fig. 3 and *SI Appendix*, Table S6) and their higher percentage of (semi)deciduous forests (47) would make these regions more sensitive to tree mortality through carbon starvation. This could explain why their trend in TAC is driven by increased drought duration, compared to the TAC trend in the north-western regions 1 and 3 being driven only by frequency. In the south-eastern and eastern subregions (2 and 12, respectively), this loss of stability is linked to increased drought intensity. Both regions consist mainly of moist evergreen forests (47), suggesting a high sensitivity to hydraulic failure and high-intensity droughts. The sensitivity of the north-eastern region 11 to longer droughts might also be related to its relatively high seasonality (Fig. 3 and *SI Appendix*, Table S6), indicating the occurrence of tree species with more resistant xylem (43) that could make them more sensitive to carbon starvation as well, similar to the southern regions.

On the other hand, in the central and northern regions (5, 6, 7, 9, and 10, respectively), and in the southern region 8, we do not find clear indicators of drought-related drivers of slowing down. In these central models, the drought-related variables only show significant decreasing effects, while they were not significant in the southern model (*SI Appendix*, Table S1). It is worth noting that subregion 8 extended beyond the study region, meaning that the lower half of this region was not represented in the model results. Both central regions (5 and 6) have experienced a high number of drought events, and ranked among the regions with the highest average drought intensity and duration among all regions (*SI Appendix*, Table S6). As a result, their limited responsiveness to various types of droughts might be attributed to their extensive prior exposure to droughts, and thus, to a possible preprogrammed adaptive mechanism against such events.

A limitation of our models is that, by using TAC derived from EVI time series, we assume that a decreased greenness of the vegetation not linked to seasonality indicates decreased vitality of the forest. This assumption is not problematic in areas where tree species cope with droughts by mainly focusing on embolism resistance. However, some tropical tree species respond to changing precipitation regimes by shifting their investment from stem growth to root growth without a decrease in their total productivity (50). It is also important to note that TAC is an indicator and not a direct measurement of stability. The assumption of a linear relationship between TAC and stability may not hold in a multidimensional system such as the Amazon, and may therefore provide an incomplete picture of ecosystem dynamics. However, the observed slowing down of EVI does indicate clear changes in the functioning of the ecosystem. Additionally, our analysis omitted pixels significantly affected by human activity. Nevertheless, we anticipate that anthropogenic disturbances would likely amplify the adverse effects of extreme droughts on the slowing down response of the forest (51). Moreover, the length of the time series is restricted, limiting its representation of long-term trends in the Amazon forest. However, since the time period used in this study includes multiple widespread drought events, we were able to capture the short-term responses to these recurrent events.

To summarize, our findings reveal a correlation between an increased TAC and recurrent extreme drought occurrences across the Amazon forest. The observed slowing down patterns, as discussed here, find support in other remote sensing studies (4, 5), underscoring their reliability. However, the challenge to correctly interpret these remotely sensed patterns and their driving forces remains, illustrated by the low pseudo-R^2 values of the models, which indicate that a great part of the variability within the TAC trend remains unexplained. The next crucial step involves using mechanistic models to unravel the causality behind these relationships.

Based on our analyses, we speculate that the predicted increase in drought intensity and duration will likely expand the forest areas experiencing critical slowing down, particularly in the more seasonal north- and south-eastern regions. The internal rain cycle in these areas may trigger a cascading effect, potentially leading to further slowing down in other parts of the Amazon forest, with implications for global effects on other tipping points (52, 53). Thus, safeguarding these mature forests and mitigating additional global warming should be primary concerns of international importance. Recognizing the pivotal role of indigenous peoples and traditional communities in preserving these forests and fulfilling commitments to combat climate change is crucial (54, 55).

Materials and Methods

Satellite Imagery. The delineation of the Amazon forest was adopted from ref. 56. Monthly images of the Enhanced Vegetation Index (EVI) over the Amazon forest were derived over the period 2001 to 2019 from the daily MODIS MCD43C4 product with a spatial resolution of 0.05° (23), following ref. 20, using Eq. **1**:

$$\mathrm{EVI} = 2.5 \times \frac{(\mathrm{NIR} - \mathrm{RED})}{(\mathrm{NIR} + 6 \times \mathrm{RED} - 7.5 \times \mathrm{BLUE} + 1)}, \qquad [\mathbf{1}]$$

with NIR, RED, and BLUE the surface reflectance values of the near-infrared, red, and blue MODIS bands. We used EVI instead of Normalized Difference Vegetation Index (NDVI) time series because the former is more sensitive to canopy variations in high biomass regions (57). Data masking and preprocessing followed ref. 14. We excluded pixels from the time series when they had a low Bidirectional Reflectance Distribution Function (BRDF) inversion quality (50% or more fill values) or when they were classified as outliers (58). Afterward, pixels with more than 10% missing values in their time series were masked (20). In order to decrease the probability of anthropogenic influences on the drought response of the Amazon forest, the analysis focused on native forest landscapes (59) with a tree cover higher than 60% as derived from the MODIS MOD44B vegetation continuous fields product (60), and burnt areas derived from the MODIS MCD64A1 burned areas product (61) were also masked out.

For the comparison with the VOD, we used the Ku-band product from the Vegetation Optical Depth Climate Archive (VODCA) dataset (62). It has a resolution of 0.25°, and the pixels were masked using the criteria of Boulton et al. (4) of ≤80% evergreen broadleaf fraction and the presence of human land use according to the MODIS Land Cover Type product in 2001 (4, 63).

The kernel Normalized Difference Vegetation Index (kNDVI) was calculated from the same MODIS MCD43C4 product (23) following ref. 28, using Eq. **2**:

$$\mathrm{kNDVI} = \tanh\left(\left(\frac{\mathrm{NIR} - \mathrm{RED}}{2 \times \sigma}\right)^2\right), \qquad [\mathbf{2}]$$

with NIR and RED as the surface reflectance values of the near-infrared and red MODIS bands and σ as a length-scale parameter to represent the sensitivity of the index to sparsely/densely vegetated regions. We calculated σ per pixel as the temporal median of 0.5 × (NIR + RED), following ref. 28, and used the quality bands to remove pixels from the time series when they had a low BRDF inversion quality. We then removed all pixels that were masked out in the EVI product. The

kNDVI is more resistant to saturation and is more robust to noise and stability across spatial and temporal scales, compared to the NDVI and EVI (28).

Drought Events. For precipitation data, we used the monthly TerraClimate dataset from 1980 to 2019, with a spatial resolution of 0.041°, which is 4 km at the equator (26). The precipitation data were rescaled using bilinear interpolation to the same resolution of the EVI data. We calculated the precipitation seasonality as the Seasonality Index following Walsh and Lawler (38) and the interannual variability of precipitation as the coefficient of variation of the annual mean precipitation values following ref. 39.

Extreme droughts were defined both spatially and temporally using cumulative water deficit (CWD) anomalies, following ref. 14. We calculated the CWD over the Amazon forest from precipitation time series from 1980 to 2019 (26) according to Aragão et al. (9), assuming a fixed evapotranspiration of 100 mm per month. From this CWD dataset, we calculated the mean and SD of CWD per month. Standardized anomalies were then calculated per pixel by subtracting the mean from the pixel value and dividing the result by the SD. CWD anomalies below −1.96 are significantly drier than average (with $P < 0.05$). We defined extreme drought periods as starting with at least 2 mo of significantly dry CWD anomalies and ending when the anomaly gets positive, similar to how Anderson et al. (64) defined drought periods using the Standardized Precipitation Index (SPI). Because we used a fixed evapotranspiration value, the CWD anomalies in this study represent meteorological droughts and not hydrological droughts. Extreme wet periods were defined similarly by calculating cumulative water excess (CWE) anomalies (14, 32). We used a nonstandardized drought metric over the SPI to define our drought events because the tropical forest response to droughts is known to be decoupled from standardized drought indices (65).

Drought frequency is the number of droughts that occurred during a certain period. Drought intensity and duration are calculated per drought period. Drought intensity is calculated as the absolute value of the most negative CWD anomaly value during the drought period. Drought duration is defined as the number of months in the drought period. The average intensity and duration of droughts per pixel are determined by calculating the mean values of intensity and duration for all droughts occurring within the pixel during the specified period. Wet severity is the absolute value of the sum of all CWE anomaly values within a wet period. We include multiple drought characteristics to achieve a quantitative picture of the drought impact on the tropical forest ecosystem (66).

TAC. The EVI time series were detrended and deseasonalized using STL decomposition (seasonal and trend decomposition using Loess) (67). We defined the time window used to calculate the long-term trend at 19 mo and the seasonal window at 13 mo. The remainder of the decomposed EVI time series was used to calculate the lag-1 autocorrelation with a moving window length of 5 y (60 mo) (4). The results were robust when using alternative moving window lengths of 3 or 7 y (*SI Appendix*, Fig. S2 and Table S3). In the EVI TAC calculation, we did not use a fixed seasonal window in the STL decomposition like Boulton et al. (4) did. If a drought would cause a permanent change in the seasonality amplitude or offset of the time series, using a fixed seasonality would cause anomalies in the remainder component and thus in the TAC that are not related to a changed stability per se (20). We also did not control for longer cycles such as El Niño Southern Oscillation (ENSO) that might influence the precipitation and drought regimes of the Amazon, as we are interested in their impact on the critical slowing down response of the Amazon. This resulted in 70,336 pixels that could be included in the following analyses. The same process was followed for the kNDVI time series, resulting in 107,345 pixels with a nonmasked trend in TAC (*SI Appendix*, Fig. S4). The trend in TAC was calculated as the slope of the linear regression of the TAC time series from 2001 to 2019.

For the comparison with the VOD, we calculated the EVI and VOD TAC over the same time period 2001 to 2016, and we did calculate the VOD TAC using a fixed seasonality following the method of Boulton et al. (4) (*SI Appendix*, Fig. S3). The VOD TAC looks different from that of Boulton et al. (4) because of the different time period used in the analysis. Recent research found that the merging of data from multiple sensors done to produce the VODCA dataset induces strong biases on critical slowing down indicators (68); hence, these data are not used in the further models.

The temporal dynamics of the EVI TAC can be driven by two processes: 1) the changes in the stability of the system that influence the return rate after external perturbations and 2) the confounding effects of the changes in TAC of the climate driver that directly affect the EVI TAC (6, 20, 69). In this study, we are only interested in the first process, so we checked whether the confounding effect was present in our data. We derived the TAC of the CWD anomalies time series in the same way as those of the EVI time series, and calculated the overall trend in TAC to represent the TAC dynamics of the climate driver. An increasing trend in the TAC trends of the CWD anomalies would point to a systematic change in the drought regime. This could be a change in the drought frequency, intensity, or duration. If the confounding effect would be present, we would expect a positive relationship between the TAC trends of the EVI and CWD anomalies. However, our data did not show this significant positive relationship (*SI Appendix*, Fig. S10). Therefore, we assume that the original EVI TAC time series can be used to investigate the changes in the Amazon forest stability that might lead to critical slowing down.

Variance. In order to quantify the trend in variance, we also used the remainder of the decomposed EVI time series to calculate the SD with a moving window length of 5 y (60 mo). The trend in EVI SD over 2001 to 2019 had a slight but significant positive relationship ($R^2 = 0.02$, $P < 0.001$) with the trend in EVI TAC and showed a similar mean trend with the minimal value reached in May 2013, followed by a significant increasing trend until 2019 (*SI Appendix*, Fig. S8).

Sensitivity of EVI TAC to Drought Events. To visualize the sensitivity of the EVI TAC to drought events, we first calculated the mean time series of the significant CWD anomalies across the whole Amazon to find the most widespread drought months according to our drought definition. We used a threshold of at least three consecutive months of mean values below −0.08 to define a widespread drought event, resulting in three drought events from June to December 2005 ("2005 drought"), September 2009 to January 2010 ("2010 drought") and September 2015 to May 2016 ("2015 drought") (*SI Appendix*, Fig. S5). For each of these droughts, we then calculated the mean EVI TAC time series for all pixels that experienced at least 1 mo of that drought, and we can see peaks in the time series of the drought pixels during the associated drought period (colored arrows in *SI Appendix*, Fig. S5). We also calculated the difference in the average time series of all pixels affected and unaffected by the three widespread drought events. Particularly for the 2010 and 2015 droughts, this illustrates the increase in the mean TAC of the affected pixels compared to their nondrought counterparts (*SI Appendix*, Fig. S5). We then divided all pixels into three different drought history categories, depending on their total drought duration (0 mo, 1 to 10 mo, and more than 10 mo). To account for the different number of pixels in each category, we calculated the mean EVI TAC trend value of 100 randomly chosen pixels per category, and we repeated this procedure 1,000 times for each category to make sure that the sampling was not leading to spurious results. We then plotted boxplots of the 1,000 mean EVI TAC trends per category (*SI Appendix*, Fig. S6). We used the total drought duration both in the whole time period, 2001 to 2019, and in the period when the mean EVI TAC across the Amazon increased, 2013 to 2019 (Fig. 1). For both time periods, the TAC trend of the no-drought group was significantly different from the medium- and long-drought histories according to Kruskal–Wallis and post hoc Dunn tests (70, 71). These boxplots show that pixels that experienced long droughts have a more increasing trend in TAC than those that experienced no droughts, especially when the droughts occurred more recent (*SI Appendix*, Fig. S6). Both figures indicate that the raw EVI TAC values are sensitive enough to detect the ecosystem response to extreme drought events, even when spatial autocorrelation and the climatic diversity across the Amazon are not taken into account.

Time-Varying EVI TAC Trend. The Amazon forest is a very complex system, which is not easily captured using only one parameter. As an additional line of support for our interpretation that the Amazon is losing stability due to increased drought occurrences, we applied a Bayesian DLM to estimate time-varying EVI TAC, using the available code of Liu et al. (37). The Bayesian DLM consists of an observation equation and a state evolution equation, and estimates the time-varying TAC from the EVI and precipitation time series, to also account for the temporal variation in climate forcing. 97% of all pixels had an increasing linear trend in the time-varying EVI TAC over 2001 to 2019 (*SI Appendix*, Fig. S9). We used the same methodology as before to show the sensitivity of the TAC trend to different drought histories. For each drought history category, we randomly selected 100 pixels, took their mean, and repeated this procedure 1,000 times. Pixels that experienced more drought months had significantly higher time-varying EVI TAC trends (*SI Appendix*, Fig. S9).

Spatial Simultaneous Autoregressive Lag Models. We performed linear regressions to analyze the relationship between the extreme drought occurrences and the potential critical slowing down of the Amazon forest vegetation over the period 2001 to 2019. The trend in TAC was used as the response variable in the models, while drought and environmental characteristics were included as explanatory variables. To address the proposed research question that aims to identify which drought characteristic has the most significant impact on the Amazon's slowing down response, we considered drought frequency, average intensity, and average duration as relevant factors. Furthermore, we included three environmental variables that are known to impact the stability of tropical forests based on previous findings. Consistent with prior research (39, 72), we expected that higher seasonality would decrease the stability of the Amazon. The impact of higher interannual variability of precipitation on the stability of tropical forests has been reported to be both positive and negative, depending on the time period included and the regions considered (14, 21, 39). Finally, we included the total severity of extreme wet periods in our analysis. Previous research has suggested that extreme wet periods could mitigate the negative effects of subsequent extreme drought events (14, 32). Our objective was to investigate whether this also holds true when investigating the slowing down response of the Amazon. We did not include more variables in the analysis to keep the main model focused on drought-related drivers. However, we additionally created a separate model that included extra environmental variables describing the elevation (73) and the soil sand and clay content (74) across the Amazon to test whether adding extra variables would improve the explanatory power of the model (*SI Appendix*, Table S7). Adding extra environmental variables improved the model fit (lower AIC) but did not change the significance of any of the drought-related drivers compared to the main model (*SI Appendix*, Table S7).

We checked that our model met all the assumptions of a linear model. These assumptions are linearity of the data, normality of the residuals, homogeneity of residuals variance, and independence of the error terms. A Moran's I test indicated the presence of spatial autocorrelation in the residuals of the fitted linear models, which can affect the estimates of the model coefficients. The variogram pointed to a range of spatial correlation between pixels of 9.5 km. We used a Lagrange Multiplier Diagnostic for spatial dependence to find a substitute model structure for the linear models, and the SSALM was found to decrease the model AIC the most (31, 75, 76). The SSALM assumes that the autoregressive process only occurs in the response variable, which is the trend in TAC. A neighborhood structure was created by defining all pixels closer than the range as neighbors and assigning higher weights to closer neighbors in a spatial weights matrix (W). These weights ranged from 0.13 to 1.00. The SSALM includes a term for the spatial autocorrelation in the response variable (ρWY, with ρ as the autoregression coefficient), together with the standard term for the n explanatory variables and errors ($X_n\beta_n + \varepsilon$) used in ordinary least squares (OLS) regression (31):

$$Y = \rho WY + X_1\beta_1 + X_2\beta_2 + \ldots\ldots + X_n\beta_n + \varepsilon.$$

Fitting the SSALM to our data significantly improved our models by decreasing the AIC. The Nagelkerke R^2 was included as a measure of goodness of fit (77).

We included all three drought characteristics (drought frequency, average drought duration, and average drought intensity), together with the total wet severity, the precipitation seasonality, and the interannual variability of the precipitation in the model as explanatory variables (Fig. 2 and *SI Appendix*, Fig. S7). We included two-way interactions between the drought frequency and all other variables since we expected their effects would change depending on the number of drought occurrences. This resulted in all variance inflation factors (VIFs) having values below five. In the main model, the drought characteristics were calculated on the same period as the EVI time series (January 2001 until December 2019). However, the results did not change when the time period of the drought characteristics was extended five, ten, or 15 y earlier or when a shorter or longer moving window was used to calculate the TAC (*SI Appendix*, Tables S2 and S3). When we repeated the analysis including only the pixels with a significant trend in TAC that did not exhibit a significant trend in SD in the opposite direction (5), following the theory that an increase in TAC cannot serve as evidence of slowing down if there is no corresponding increase in variance (22), we were left with 37,990 or 54% out of 70,336 pixels (*SI Appendix*, Fig. S8). The only difference in the SSALM output from the original model was that the main effect of drought duration did not have a significant effect on the TAC trend anymore (*SI Appendix*, Table S4). When we repeated the analysis using the kNDVI TAC trend as a response variable, we also got similar results (*SI Appendix*, Table S5). The main difference between the models was that the main effect of drought frequency was not significant in the EVI model, but significantly negative in the kNDVI model. The destabilizing effects of more intense, longer, and more frequent and intense droughts are shown in the kNDVI model as well.

Regional Models. We used a subdivision of the Amazon into 13 woody plant subregions, following Silva-Souza and Souza (35). They used data on woody species composition from 301 assemblages and performed unconstrained ordination, interpolation, and clustering techniques to identify these 13 woody subregions. The variation in their subregions could partly be explained by human factors, spatial structure, and environmental variables. The SSALM was iteratively run separately for each subregion to look at the spatial variation of the drought and climatic effects on the TAC trend (*SI Appendix*, Table S1). Because each subregion was composed of a different amount of pixels, we randomly selected 1,200 pixels from each subregion to use in the models. We used 1,200 pixels as this was the number of pixels included in the one-to-smallest subregion. Subregion 13 only included 562 pixels and is the only subregion for which the model was run with fewer pixels. In Fig. 3, drought frequency, intensity, and duration were defined as drivers of slowing down in a region when they had at least one main or interaction effect that significantly increased the TAC trend and no effects that significantly decreased the TAC trend. *SI Appendix*, Table S6 shows the variation in drought occurrences and environmental variables in each of the subregions.

Text. We used the assistance of the Large Language Model, ChatGPT, to improve the fluency and readability of the text.

Data, Materials, and Software Availability. TIF files and R scripts data have been deposited in Figshare and GitHub (https://figshare.com/s/0363ff12d5bee640524b and https://github.com/jvanpassel/amazon_droughts) (78, 79).

ACKNOWLEDGMENTS. J.V.P. received funding from the Research Foundation Flanders (FWO) (grant number G063420N). P.N.B. received funding from the Research Foundation Flanders (FWO) (grant number G0F6922N). This work was supported by the Serrapilheira Institute (grant number Serra-1709-18983).

Author affiliations: [a]Division Forest, Nature and Landscape, KU Leuven, Leuven 3001, Belgium; [b]KU Leuven Plant Institute, KU Leuven, Leuven 3001, Belgium; [c]Department of Plant Biology, University of Campinas, Campinas-SP 13083-970, Brazil; [d]Department Geoscience & Remote Sensing, Delft University of Technology, Delft 2600, The Netherlands; [e]Center for Meteorological and Climatic Research Applied to Agriculture, University of Campinas, Campinas-SP 13083-970, Brazil; [f]Interdisciplinary Environmental Studies Laboratory, Department of Physics, Federal University of Santa Catarina, Florianópolis, SC 88040-900, Brazil; [g]Plant Ecology, University of Bayreuth, Bayreuth 95447, Germany; and [h]Flemish Institute for Technological Research (VITO), Mol 2400, Belgium

Author contributions: J.V.P., K.V.M., and B.S. designed research; J.V.P. performed research; J.V.P., P.N.B., S.L., W.d.K., K.V.M., and B.S. analyzed data; and J.V.P., P.N.B., S.L., B.F.R., M.H., T.C., W.d.K., K.V.M., and B.S. wrote the paper.

1. Y. Pan *et al.*, A large and persistent carbon sink in the world's forests. *Science* **333**, 988–993 (2011).
2. T. R. Feldpausch *et al.*, Tree height integrated into pantropical forest biomass estimates. *Biogeosciences* **9**, 3381–3403 (2012).
3. H. ter Steege *et al.*, Biased-corrected richness estimates for the Amazonian tree flora. *Sci. Rep.* **10**, 1–13 (2020).
4. C. A. Boulton, T. M. Lenton, N. Boers, Pronounced loss of Amazon rainforest resilience since the early 2000s. *Nat. Clim. Change* **12**, 271–278 (2022).
5. T. Smith, D. Traxl, N. Boers, Empirical evidence for recent global shifts in vegetation resilience. *Nat. Clim. Change* **12**, 477–484 (2022).
6. G. Forzieri, V. Dakos, N. G. McDowell, A. Ramdane, A. Cescatti, Emerging signals of declining forest resilience under climate change. *Nature* **608**, 534–539 (2022).
7. M. Scheffer *et al.*, Early-warning signals for critical transitions. *Nature* **461**, 53–59 (2009).
8. W. M. Hammond *et al.*, Global field observations of tree die-off reveal hotter-drought fingerprint for Earth's forests. *Nat. Commun.* **13**, 1761 (2022).
9. L. E. O. C. Aragão *et al.*, Spatial patterns and fire response of recent Amazonian droughts. *Geophys. Res. Lett.* **34**, 1–5 (2007).
10. S. L. Lewis, P. M. Brando, O. L. Phillips, G. M. F. Van Der Heijden, D. Nepstad, The 2010 Amazon drought. *Science* **331**, 554 (2011).

11. J. C. Jimenez *et al.*, Spatio-temporal patterns of thermal anomalies and drought over tropical forests driven by recent extreme climatic anomalies. *Philos. Trans. R Soc. B Biol. Sci.* **373**, 20170300 (2018).
12. IPCC, "Summary for Policymakers" in *Climate Change 2021: The Physical Science Basis. Contribution of Working Group I to the Sixth Assessment Report of the Intergovernmental Panel on Climate Change*, V. Masson-Delmotte *et al.*, Eds. (Cambridge University Press, Cambridge, United Kingdom and New York, In press, 2021), p. 42.
13. S. Tao *et al.*, Increasing and widespread vulnerability of intact tropical rainforests to repeated droughts. *Proc. Natl. Acad. Sci. U.S.A.* **119**, e2116626119 (2022).
14. J. Van Passel *et al.*, Climatic legacy effects on the drought response of the Amazon rainforest. *Glob. Chang. Biol.* **28**, 5808–5819 (2022), 10.1111/gcb.16336.
15. T. R. Feldpausch *et al.*, Amazon forest response to repeated droughts. *Global Biogeochem. Cycles* **30**, 964–982 (2016).
16. N. Wunderling *et al.*, Recurrent droughts increase risk of cascading tipping events by outpacing adaptive capacities in the Amazon rainforest. *Proc. Natl. Acad. Sci. U.S.A.* **119**, e2120777119 (2022).
17. H. Held, T. Kleinen, Detection of climate system bifurcations by degenerate fingerprinting. *Geophys. Res. Lett.* **31**, 1–4 (2004).
18. V. Dakos *et al.*, Methods for detecting early warnings of critical transitions in time series illustrated using simulated ecological data. *PLoS One* **7**, 1–20 (2012).
19. Y. Liu, M. Kumar, G. G. Katul, A. Porporato, Reduced resilience as an early warning signal of forest mortality. *Nat. Clim. Change* **9**, 880–885 (2019).
20. J. Verbesselt *et al.*, Remotely sensed resilience of tropical forests. *Nat. Clim. Change* **6**, 1028–1031 (2016).
21. T. Smith, N. Boers, Global vegetation resilience linked to water availability and variability. *Nat. Commun.* **14**, 498 (2023).
22. P. D. Ditlevsen, S. J. Johnsen, Tipping points: Early warning and wishful thinking. *Geophys. Res. Lett.* **37**, 1–4 (2010).
23. C. Schaaf, Z. Wang, MCD43C4 MODIS/Terra+Aqua BRDF/Albedo Nadir BRDF-Adjusted Ref Daily L3 Global 0.05Deg CMG V006 [Data set] (2015). https://doi.org/10.5067/MODIS/MCD43C4.006. Accessed 1 May 2020.
24. W. R. L. Anderegg, L. D. L. Anderegg, C. Huang, Testing early warning metrics for drought-induced tree physiological stress and mortality. *Glob. Chang. Biol.* **25**, 2459–2469 (2019).
25. D. Wu *et al.*, Reduced ecosystem resilience quantifies fine-scale heterogeneity in tropical forest mortality responses to drought. *Glob. Chang. Biol.* **28**, 2081–2094 (2022).
26. J. T. Abatzoglou, S. Z. Dobrowski, S. A. Parks, K. C. Hegewisch, TerraClimate, a high-resolution global dataset of monthly climate and climatic water balance from 1958–2015. *Sci. Data* **5**, 1–12 (2018).
27. S. Tao *et al.*, Little evidence that Amazonian rainforests are approaching a tipping point. *Nat. Clim. Chang.* **13**, 1317–1320 (2023).
28. G. Camps-Valls *et al.*, A unified vegetation index for quantifying the terrestrial biosphere. *Sci. Adv.* **7**, eabc7447 (2021).
29. M. Longo *et al.*, Ecosystem heterogeneity and diversity mitigate Amazon forest resilience to frequent extreme droughts. *New Phytol.* **219**, 914–931 (2018).
30. B. M. Flores, A. Staal, Feedback in tropical forests of the Anthropocene. *Glob. Chang. Biol.* **28**, 5041–5061 (2022).
31. W. D. Kissling, G. Carl, Spatial autocorrelation and the selection of simultaneous autoregressive models. *Global Ecol. Biogeogr.* **17**, 59–71 (2007).
32. E. J. L. Esteban, C. V. Castilho, K. L. Melgaço, F. R. C. Costa, The other side of droughts: Wet extremes and topography as buffers of negative drought effects in an Amazonian forest. *New Phytol.* **229**, 1995–2006 (2021).
33. J. Aguirre-Gutiérrez *et al.*, Functional susceptibility of tropical forests to climate change. *Nat. Ecol. Evol.* **6**, 878–889 (2022).
34. A. C. Bennett *et al.*, Sensitivity of South American tropical forests to an extreme climate anomaly. *Nat. Clim. Chang.* **13**, 967–974 (2023).
35. K. J. P. Silva-Souza, A. F. Souza, Woody plant subregions of the Amazon forest. *J. Ecol.* **108**, 2321–2335 (2020).
36. G. Sugihara *et al.*, Detecting causality in complex ecosystems. *Science* **338**, 496–500 (2012).
37. Y. Liu, M. Kumar, G. G. Katul, A. Porporato, Reduced resilience as an early warning signal of forest mortality. *Nat. Clim. Chang.* **9**, 880–885 (2019).
38. P. D. Walsh, D. M. Lawler, Rainfall seasonality: Description, spatial patterns and change through time. *Weather* **36**, 201–208 (1981).
39. C. Ciemer *et al.*, Higher resilience to climatic disturbances in tropical vegetation exposed to more variable rainfall. *Nat. Geosci.* **12**, 174–179 (2019).
40. H. Zhang, D. F. T. Hagan, R. Dalagnol, Y. Liu, Forest canopy changes in the southern Amazon during the 2019 fire season based on passive microwave and optical satellite observations. *Remote Sens.* **13**, 2238 (2021).
41. E. Bousquet, A. Mialon, N. Rodriguez-Fernandez, S. Mermoz, Y. Kerr, Monitoring post-fire recovery of various vegetation biomes using multi-wavelength satellite remote sensing. *Biogeosciences* **19**, 3317–3336 (2022).
42. A. Esquivel-Muelbert *et al.*, Compositional response of Amazon forests to climate change. *Glob. Chang. Biol.* **25**, 39–56 (2019).
43. J. V. Tavares *et al.*, Basin-wide variation in tree hydraulic safety margins predicts the carbon balance of Amazon forests. *Nature* **617**, 111–117 (2023).
44. L. Rowland *et al.*, Death from drought in tropical forests is triggered by hydraulics not carbon starvation. *Nature* **528**, 119–122 (2015).
45. A. Esquivel-Muelbert *et al.*, Tree mode of death and mortality risk factors across Amazon forests. *Nat. Commun.* **11**, 5515 (2020).
46. N. McDowell *et al.*, Mechanisms of plant survival and mortality during drought: Why do some plants survive while others succumb to drought? *New Phytol.* **178**, 719–739 (2008).
47. K. G. Dexter *et al.*, Inserting tropical dry forests into the discussion on biome transitions in the tropics. *Front. Ecol. Evol.* **6**, 104 (2018).
48. N. Butt *et al.*, Shifting dynamics of climate-functional groups in old-growth Amazonian forests. *Plant Ecol. Diversity* **7**, 267–279 (2014).
49. G. Vico, D. Dralle, X. Feng, S. Thompson, S. Manzoni, How competitive is drought deciduousness in tropical forests? A combined eco-hydrological and eco-evolutionary approach. *Environ. Res. Lett.* **12**, 065006 (2017).
50. K. J. Feeley, S. Joseph Wright, M. N. Nur Supardi, A. R. Kassim, S. J. Davies, Decelerating growth in tropical forest trees. *Ecol. Lett.* **10**, 461–469 (2007).
51. H. Wang *et al.*, Anthropogenic disturbance exacerbates resilience loss in the Amazon rainforests. *Glob. Chang. Biol.* **30**, e17006 (2023).
52. T. Liu *et al.*, Teleconnections among tipping elements in the Earth system. *Nat. Clim. Chang.* **13**, 67–74 (2023).
53. N. Wunderling *et al.*, Global warming overshoots increase risks of climate tipping cascades in a network model. *Nat. Clim. Chang.* **13**, 75–82 (2023).
54. C. Levis *et al.*, Help restore Brazil's governance of globally important ecosystem services. *Nat. Ecol. Evol.* **4**, 172–173 (2020).
55. D. Prioli Duarte, C. A. Peres, E. F. C. Perdomo, A. Guizar-Coutiño, B. W. Nelson, Reducing natural vegetation loss in Amazonia critically depends on the formal recognition of indigenous lands. *Biol. Conserv.* **279**, 109936 (2023).
56. D. M. Olson *et al.*, Terrestrial ecoregions of the world: A new map of life on Earth. *Bioscience* **51**, 933–938 (2001).
57. A. Huete *et al.*, Overview of the radiometric and biophysical performance of the MODIS vegetation indices. *Remote Sens. Environ.* **83**, 195–213 (2002).
58. L. Eklundh, P. Jönsson, Timesat 3.3 Software Manual (2017), pp. 1–92.
59. P. Potapov *et al.*, Mapping the World's intact forest landscapes by remote sensing. *Ecol. Soc.* **13**, 1–16 (2008).
60. C. DiMiceli *et al.*, MOD44B MODIS/Terra Vegetation Continuous Fields Yearly L3 Global 250m SIN Grid V006 [Data set] (2015). https://doi.org/10.5067/MODIS/MOD44B.006. Accessed 1 May 2020.
61. L. Giglio, C. Justice, L. Boschetti, D. Roy, MCD64A1 MODIS/Terra+Aqua Burned Area Monthly L3 Global 500m SIN Grid V006 [Data set] (2015). https://doi.org/10.5067/MODIS/MCD64A1.006. Accessed 1 May 2020.
62. L. Moesinger *et al.*, The global long-term microwave Vegetation Optical Depth Climate Archive (VODCA). *Earth Syst. Sci. Data* **12**, 177–196 (2020).
63. M. Friedl, MCD12C1 MODIS/Terra+Aqua Land Cover Type Yearly L3 Global 0.05Deg CMG V006 [Data set] (2015). https://doi.org/10.5067/MODIS/MCD12C1.006. 4 January 2023.
64. L. O. Anderson *et al.*, Vulnerability of Amazonian forests to repeated droughts. *Philos. Trans. R Soc. B Biol. Sci.* **373**, 1–13 (2018).
65. C. S. Zang *et al.*, Standardized drought indices in ecological research: Why one size does not fit all. *Glob. Chang. Biol.* **26**, 322–324 (2020).
66. Z. Zhang, X. Li, The resilience of ecosystems to drought. *Glob. Change Biol.* **29**, 3517–3518 (2023).
67. R. B. Cleveland, W. S. Cleveland, J. E. McRae, I. Terpenning, STL: A seasonal-trend decomposition procedure based on Loess. *J. Off. Statistics* **6**, 3–73 (1990).
68. T. Smith *et al.*, Reliability of resilience estimation based on multi-instrument time series. *Earth Syst. Dynam.* **14**, 173–183 (2023).
69. V. Dakos, E. H. V. Nes, P. D. Odorico, M. Scheffer, Robustness of variance and autocorrelation as indicators of critical slowing down. *Ecology* **93**, 264–271 (2012).
70. W. H. Kruskal, W. A. Wallis, Use of ranks in one-criterion variance analysis. *J. Am. Statistical Assoc.* **47**, 583–621 (1952).
71. O. J. Dunn, Multiple comparisons using rank sums. *Technometrics* **6**, 241–252 (1964).
72. A. Staal *et al.*, Forest-rainfall cascades buffer against drought across the Amazon. *Nat. Clim. Chang.* **8**, 539–543 (2018).
73. NASA JPL, NASA Shuttle Radar Topography Mission Global 3 arc second [Data set] (2013). https://doi.org/10.5067/MEaSUREs/SRTM/SRTMGL3.003. 16 September 2021.
74. L. Poggio *et al.*, SoilGrids 2.0: Producing soil information for the globe with quantified spatial uncertainty. *Soil* **7**, 217–240 (2021).
75. R. Bivand, E. Pebesma, V. Gómez-Rubio, *Applied Spatial Data Analysis with R* (Springer, New York, NY, ed. 2, 2013), 10.1007/978-1-4614-7618-4.
76. P. N. Bernardino *et al.*, Uncovering dryland woody dynamics using optical, microwave, and field data–Prolonged above-average rainfall paradoxically contributes to woody plant die-off in the western Sahel. *Remote Sens.* **12**, 2332 (2020).
77. N. J. D. Nagelkerke, A note on a general definition of the coefficient of determination. *Biometrika* **78**, 691–692 (1991).
78. J. Van Passel *et al.*, Data for "Critical slowing down of the Amazon forest after increased drought occurrence". Figshare. https://figshare.com/s/0363ff12d5bee640524b. Deposited 29 September 2023.
79. J. Van Passel, Analysis and plotting scripts. GitHub. https://github.com/jvanpassel/amazon_droughts. Deposited 7 March 2024.